Met. Mater. Int., Vol. 20, No. 5 (2014), pp. 801~806
doi: 10.1007/s12540-014-5001-2

Microstructure Evolution During Continuous Cooling in Niobium Microalloyed High Carbon Steels

Zhaodong Li[1,2,*], Qilong Yong[1,], Zhengyan Zhang[1], Xinjun Sun[1], Jianchun Cao[3], Haiquan Qi[4], and Zhi Liao[2]**

[1]Central Iron and Steel Research Institute, Department of Structural Steels, Beijing 100081, China
[2]Hunan Vanlin Lianyuan Iron and Steel Company Limited, Technology Center, Loudi 417009, China
[3]Kunming University of Science and Technology, School of Materials Science and Engineering, Kunming 650093, China
[4]Guilin University of Science and Technology, School of Materials Science and Engineering, Guilin 541004, China

(received date: 1 October 2013 / accepted date: 16 January 2014)

Effects of microalloyed niobium (Nb) on the austenite decomposition behaviors and microstructure evolution during continuous cooling in the near eutectoid steels were investigated. Compared to the Nb free steel, the Nb microalloyed steel was refined with regard to polygonal ferrite grain, pearlite block and colony sizes. This was because its austenite grain size was smaller. The volume fraction of polygonal ferrite transformed was more in the Nb microalloyed steels, which indicated the eutectoid carbon content exceeded that of pure carbon steel. The spheroidization of pearlite during continuous cooling was enhanced by Nb microalloying, mainly due to a higher critical transformation temperature and the finer pearlite structure with smaller colony size and narrower interlamellar spacing. Hot deformation right above the equilibrium eutectoid temperature accelerated the spheroidization kinetics of pearlite, especially in the Nb microalloyed steel.

Keywords: alloy, phase transformation, precipitation, annealing, thermomechanical processing

1. INTRODUCTION

As a microalloying element, the effects of niobium (Nb) on the austenite recrystallization, austenite and ferrite grain refinement, and precipitation strengthening have been widely studied and applied in low carbon steels in the past half-century [1-3]. The use of microalloyed Nb was further extended in high carbon quenched and tempered steels in the last 20 years due to its effect on austenite grain refinement [1]. However, the effects of microalloyed Nb on the behaviors and microstructure of austenite decomposition in medium and high carbon steels was rarely reported and not studied in detail.

Pearlite is one of the main microstructures in medium and high carbon non-quenched and tempered steels for rail, wire, bar, rod and so on. It is also one of transitive microstructure in the medium high carbon quenched and tempered steels. Pearlite substructures are complex and the kinetics of their evolution during cooling from hot rolling or heat treatment is important for the mechanical and processing properties of pearlitic steel products. Colony is a typical substructure in pearlite, which is a region containing cementite lamella or particles of nearly the same orientation. Cementite lamella or particle spacing is an important parameter strongly related to the strength of pearlitic steel. In 1970s, Takahashi *et al.* [4] proposed another substructure in pearlite called as "block". It is a region in which ferrite orientation is nearly the same and usually comprises some colonies. This was recently confirmed using electron backscatter diffraction (EBSD) by other researchers [5,6]. It was also revealed by Takahashi *et al.* [4] that pearlite block acted as a unit of slip and fracture of pearlitic steels. Contria *et al.* [7] also confirmed that pearlite block was the cleavage unit in pearlitic steels. The sizes of those substructures are very important for the mechanical properties of pearlitic steel. The spheroidization of lamellar cementite benefits the homogeniety of microstructure and mechanical properties of medium and high carbon steel products as well as their processing properties of cold deformation or heat treatment. The spheroidization treatment is a time- and energy-consuming process. In order to shorten the production process and lower the cost, on-line spheroidization treatment for hot rolled coils during slowly cooling by adding attemperators on the coils

*Corresponding author: lizd2006@gmail.com, yongqilong@cisri.com.cn

has been employed in steel industry.

In the present study, near eutectoid steels were employed to study the effects of microalloyed Nb on austenite decomposition behaviors and microstructure during continuous cooling. In particular, cementite morphology was focused on to examine the effects of microalloyed Nb on pearlite spheroidization.

2. EXPERIMENTAL PROCEDURE

Two Nb microalloyed high carbon steels and one Nb-free high carbon steel were used in the study. 25 kg ingot was prepared by vacuum melting and casting. After hot forged to Φ40 mm bars, Φ11 mm bars were eventually obtained by hot rolling. The chemical compositions of the hot rolled bars were shown in Table 1. According to the carbon and Nb contents, the Nb-free steel for comparison study was denoted as 0.70C steel while the Nb microalloyed steels were denoted as 0.75C-0.04Nb and 0.78C-0.06Nb steels, respectively.

On-line spheroidization of the experimental steels without and with deformation after fully austenitization was studied. Firstly, to study the effects of Nb on the microstructure without hot deformation before transformation, hot rolled bars were annealed at 800 °C for 1 h, followed by furnace cooling for 90 min to 550 °C and then air cooling for 120 min to room temperature. Secondly, the couple effects of Nb addition and thermal mechanical process were studied. By using Gleeble-1500D, the specimen in size of Φ8 mm×12 mm cut from the hot rolled bars were heated and held at 760 °C for 5 min, then cooled to 730 °C at 5 °C/s. After uniaxially compressed by 20% at 730 °C, continuous cooling to 630 °C at 50 °C/h and then water quench to room temperature were conducted. During deformation at 730 °C, which was just above the equilibrium eutectoid temperatures (Ae_1) of the experimental steels with near eutectoid compositions, austenite hardening, austenite decomposition and reaustenitization possibly occurred. It would refine the sizes of austenite grain and transformed pearlite block and promote pearlite spheroidization.

In order to examine the solution of Nb(C,N), the hot rolled specimens sealed in the Ar-filled silicon tubes were reheated to different temperatures in the range from 800 to 1200 °C, then isothermally held for 2 h and finally water quenched. The Nb(C,N) precipitates in the reheated specimens were electrolytically extracted in the solution of 3 g $N(CH_3)_4Cl$, 30 ml $CH_3COCH_2COCH_3$ and 270 ml CH_3OH at 20 °C. The precipitated Nb content was measured by Inductively Coupled Plasma-Atomic Emission Spectrometry (ICP-AES). The critical transformation temperatures of the studied steels during continuous heating and cooling were measured by Formastor-II dilatometer using Φ3 mm×10 mm specimens cut from the annealed bar. The specimens were heated to 800 °C at 200 °C/h and held for 5 min, followed by cooling at 200 °C/h as well. All specimens for microstructure observations were prepared by mechanical and electrolytic polishing. After etched by 2% nital solution, the microstructure was observed using optical microscopy (OM) and scanning electron microscopy (SEM). The ferritic structure including polygonal ferrite and pearlite block in the annealed bars were characterized by electron backscatter diffraction (EBSD). The volume fraction of polygonal ferrite or pearlite was measured by point counting method. The grain size of polygonal ferrite or pearlite substructures was measured by linear intercept method. Thermo-Calc software with the database of TCFE 7 was employed to calculate the equilibrium state for reference.

Table 1. Chemical compositions (mass%) of the studied steels as hot rolled

Steel	C	Nb	N	S	P
0.70C	0.70	-	0.0028	0.0061	0.0074
0.75C-0.04 Nb	0.75	0.040	0.0019	0.0052	0.0076
0.78C-0.06 Nb	0.78	0.064	0.0011	0.0051	0.0080

3. RESULTS

3.1. Effects of microalloyed Nb on annealing microstructure

The OM and SEM micrographs of the annealing structure in the studied steels were shown in Fig. 1. As shown in Figs. 1a-c, a mixed microstructure of polygonal ferrite and lamellar pearlite was formed in the 0.70C steel. Since the 0.70C steel is indeed a hypo-eutectoid steel, the polygonal ferrite should be the proeutectoid ferrite, which usually forms along austenite grain boundaries [8]. Compared to those in Figs. 1a-c, polygonal ferrite in Figs. 1d-i became equiaxial while its amount and density increased. As summarized in Table 2, the volume fraction of polygonal ferrite in the 0.70C steel was 9.8%, agreeing well with the maximum amount of proeutectoid ferrite calculated by lever rule, based on the eutectoid composition of 0.76 mass% C calculated by Thermo-Calc. However, those in the 0.75C-0.04Nb and 0.78C-0.06Nb steels were increased to 19.8% and 16.9%, respectively. It indicated the eutectoid carbon content after Nb microalloying was higher than that (0.76 mass% C) of pure carbon steel. However, in the equilibrium calculated by Thermo-Calc, the eutectoid carbon content in the 0.1 mass% Nb microalloyed steel was increased only to about 0.77 mass%. The reason for the increment of polygonal ferrite in Nb microalloyed steels was still unknown. Furthermore, as shown in the Figs. 1c, f and i, the interlamellar spacing in the 0.75C-0.04Nb and 0.78C-0.06Nb steels was smaller than that in the 0.70C steel. This was because the higher carbon content of pearlite transformed in the Nb microalloyed steels led to a smaller interlamellar spacing [9]. It was also observed that some cementite lamellae were broken and thickened. The degeneracy or partially spheroidized area appeared more frequently in the 0.75C-0.04Nb and 0.78C-0.06Nb steels.

As summarized in Table 2, the sizes of austenite grain,

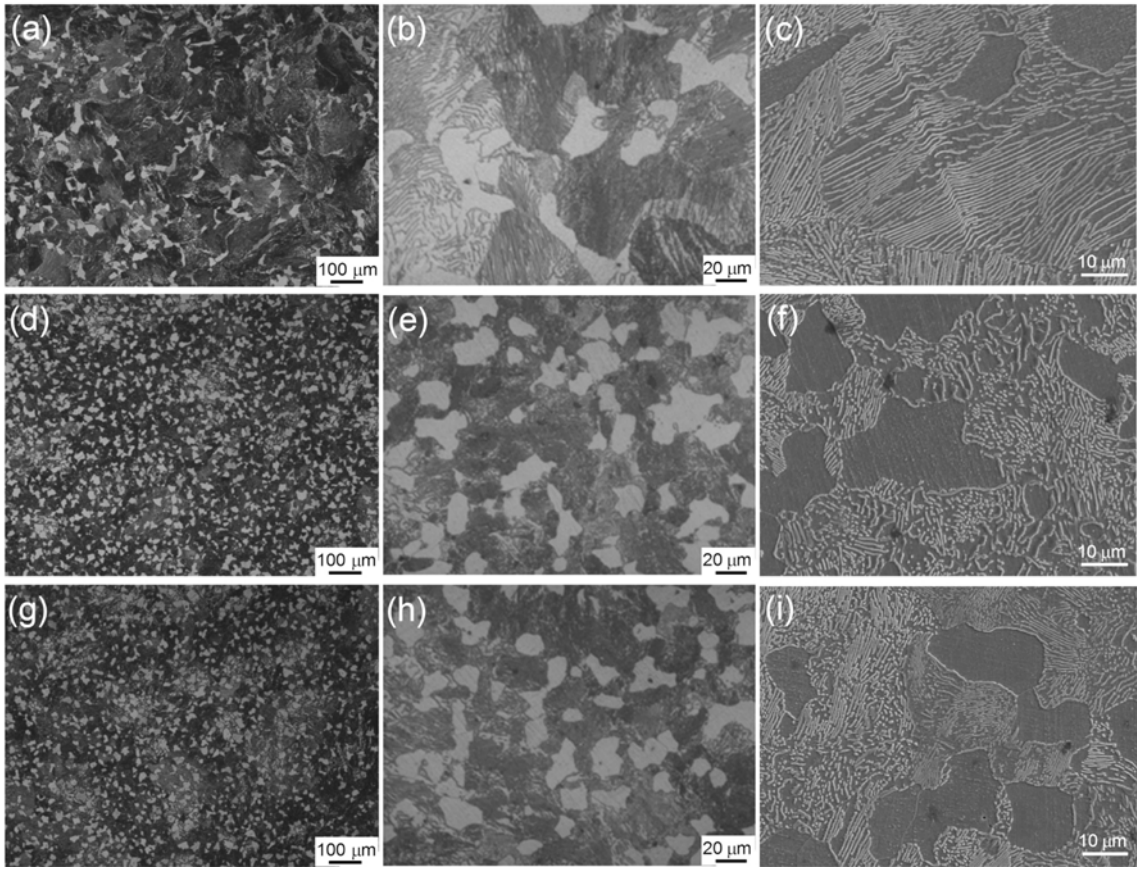

Fig. 1. OM (a, b, d, e, g, h) and SEM (c, f, i) micrographs of annealing structure in the (a-c) 0.70C, (d-f) 0.75C-0.04Nb and (g-i) 0.78C-0.06Nb steels.

Table 2. Parameters of annealing microstructure in studied steels

Steel/parameter	Austenite grain size, μm	Polygonal ferrite		Lamellar pearlite	
		Volume fraction	Grain size, μm	Block size, μm	Colony size, μm
0.70C	116	9.8%	21	68	36
0.75C-0.04 Nb	51	19.8%	14	47	19
0.78C-0.06 Nb	53	16.9%	15	-	19

pearlite colony and polygonal ferrite were refined after Nb microalloying. The austenite grain sizes were estimated according to the encircling of polygonal ferrite. Shown in Fig. 2 are EBSD image quality maps of ferritic structure with high angle boundaries (HABs) of ferrite with misorientation angle larger than 15° and low angle boundaries (LABs) of ferrite with misorientation angle of 5-15°. The gray lamellae indicated the pearlitic cementite. As shown in Fig. 2a, pearlite block of the 0.70C steel contained several pearlite colonies and some ferritic LABs, part of which corresponding to the pearlite colony boundaries. However, the size of pearlite block was smaller in the 0.75C-0.04Nb steel and less colonies and ferrtic LABs were included in the pearlite block, as shown in Fig. 2b. Due to the refinement of pearlite block and polygonal ferrite, the density of ferritic HABs in the 0.75C-0.04Nb steel was higher than that in the 0.70C steel. The refinement of pearlite block, colony and polygonal ferrite grain sizes were mainly attributed to the refinement of austenite grain size.

3.2. Effects of microalloyed Nb on on-line spheroidization of pearlite

It was observed that pearlite spheroidization during the annealing process increased after Nb microalloying. To confirm this and promote spheroidization, on-line spheroidization treatment during slowly cooling after hot rolling was carried out. The SEM results of microstructure were shown in Fig. 3. Some spheroidized pearlite was observed in the 0.70C steel as shown in Fig. 3a. However, more spheroidized pearlite was formed in the 0.75C-0.04Nb and 0.78C-0.06Nb steels as shown in Figs. 3b and 3c, respectively. The distribution of aspect ratio of pearlitic cementite in the 0.70C, 0.75C-0.04Nb and 0.78C-0.06Nb steels was shown in Figs. 3d, e and f, respec-

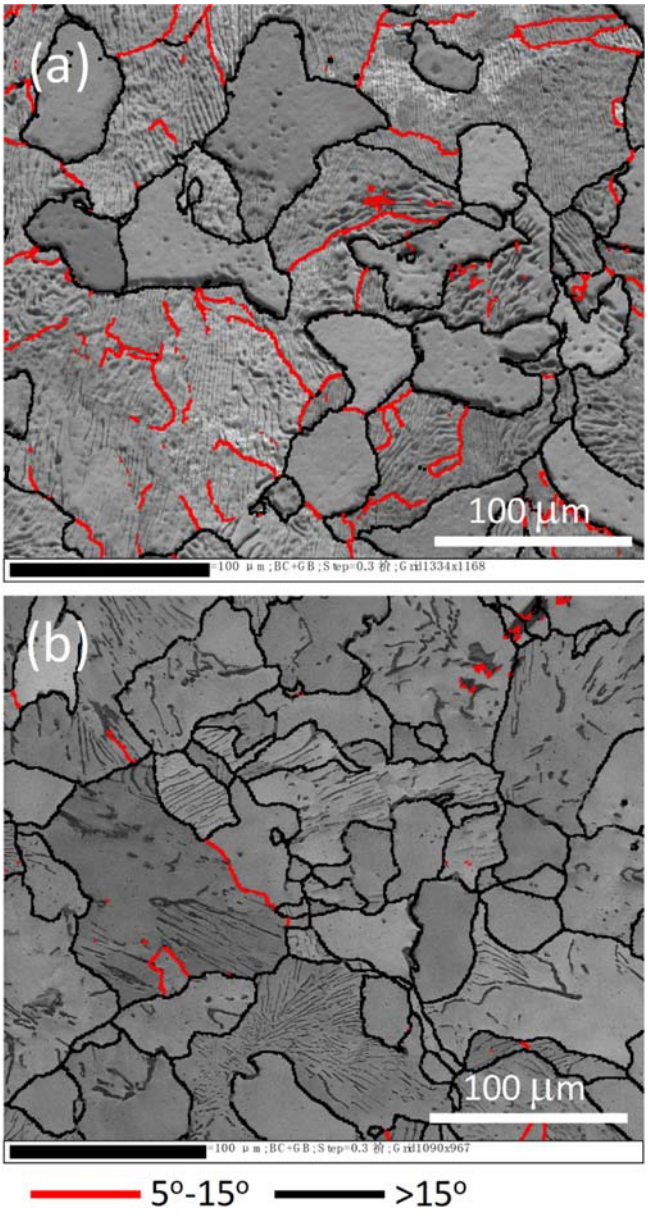

Fig. 2. EBSD image quality maps combined with ferritic boundaries, showing the ferritic boundary structure of the (a) 0.70C and (b) 0.75C-0.04Nb steels after annealed at 800 °C.

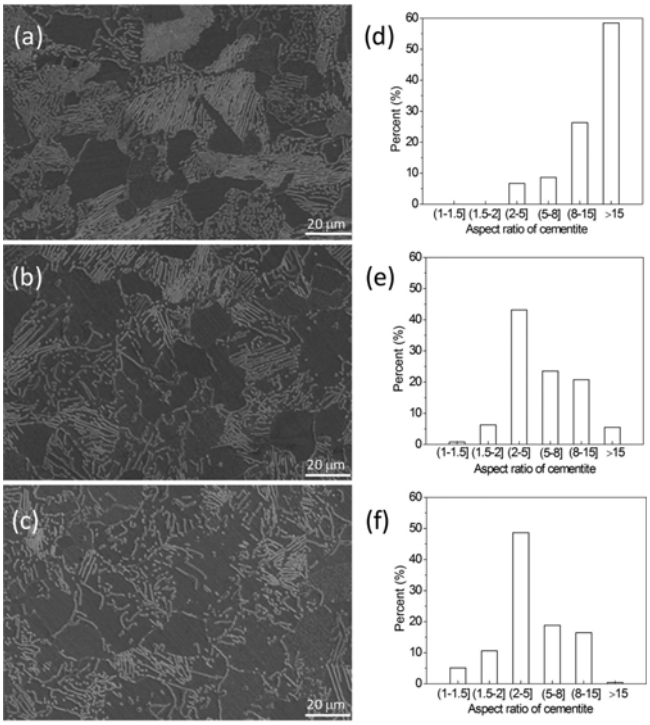

Fig. 3. SEM micrographs and the distribution of aspect ratio of pearlitic cementite in the (a) (d) 0.70C, (b) (e) 0.75C-0.04Nb and (c) (f) 0.78C-0.06Nb steels after on-line spheroidization treatment.

tively. The aspect ratio of most frequent lamellar cementite was larger than 15 in the 0.70C steel while it was changed to 2-5 in the two Nb microalloyed steels. Compared to the annealed state shown in Fig. 1, the amount of spheroidized pearlite after on-line spheroidization treatment increased.

4. DISCUSSION

4.1. States of the microadded Nb

As well known to many, Nb tends to precipitate with N and C since the solubility product of NbN and NbC in austenite is very small. Table 3 shows the ICP-AES measurement results of extracted Nb(C,N) particles in the 0.75C-0.04Nb steel. According to the composition of the alloy and precipitated

Table 3. Quantitative analysis of Nb and C contents (mass%) in different phases in the 0.75C-0.04Nb steel

Tempe-rature, ℃	Nb in Nb(C,N) (measured)	Nb in austenite (calculated)	C in austenite (calculated)	Nb in austenite (calculated by Thermo-Calc)	C in austenite (calculated by Thermo-Calc)
800	0.040	0	0.7465	0.0002	0.7455
950	0.040	0	0.7465	0.0018	0.7456
1000	0.040	0	0.7465	0.0032	0.7458
1050	0.033	0.007	0.7474	0.0056	0.7461
1100	0.029	0.011	0.7479	0.0094	0.7465
1150	0.025	0.015	0.7484	0.0152	0.7472
1200	0.020	0.020	0.7491	0.0237	0.7481

Table 4. Critical transformation temperatures (°C) of the studied steels

Steel	Ac_1	Ac_3	Ar_1	Ar_3	Ae_1	Ae_3/Ae_{cm}	Steel	Ae_1	Ae_3/Ae_{cm}
0.70C	730	760	670	700	727	735	0.70C	727	735
0.75C-0.04 Nb	730	755	680	710	727	729	0.75C	727	728
0.78C-0.06 Nb	730	755	690	725	727	731(Ae_{cm})	0.78C	727	734(Ae_{cm})

Nb(C,N), the Nb content in austenite was determined. Since the solubility product of NbN in austenite was about two orders of magnitude smaller than that of NbC at a given temperature [2,3] and no other strong nitride forming elements such as Ti and Al were added, N was supposed to be completely stabilized by Nb. Therefore, the C contents in Nb(C,N) and austenite could be calculated. As shown in Table 3, more Nb was stabilized by Nb(C,N) as the solution temperature was decreased. As a result, the Nb content in austenite was decreased and the C content in austenite was increased, which both agreed with the results calculated by Thermo-Calc. Below 1000 °C, Nb was almost completely stabilized by Nb(CN).

4.2. Effects of microalloyed Nb on the critical transformation temperatures

The experimental critical transformation temperatures during continuous heating and cooling with a rate of 200 °C/h and the calculated equilibrium transformation temperatures by Thermo-Calc were shown in Table 4. The equilibrium temperatures for ferrite or cementite to austenite transformation (Ae_3 or Ae_{cm}) were 735, 728 and 734 (Ae_{cm}) °C for the 0.70C, 0.75C, 0.78C pure carbon steels, respectively. Compared to the pure carbon steels, the Ae_3 or Ae_{cm} temperatures of the 0.75C-0.04Nb and 0.78C-0.06Nb steels were hardly changed. The Ac_3 or Ac_{cm} temperatures during the slowly heating were also hardly changed by Nb microalloying up to 0.064%. However, the Ar_3 temperatures of the 0.75C-0.04Nb and 0.78C-0.064Nb steels were at least 10 °C higher than that of the 0.70C steel. The equilibrium temperatures for eutectoid transformation (Ae_1) were about 727 °C for the 0.70C, 0.75C-0.04Nb and 0.078C-0.06Nb steels. The critical temperatures (Ac_1) for pearlite to austenite transformation during heating were also not affected by microalloyed Nb. However, the critical temperatures (Ar_1) for eutectoid transformation during cooling were increased by microalloyed Nb. In summary, the critical temperatures of continuous cooling transformation were increased by microalloyed Nb, but the critical temperatures of continuous heating transformation and equilibrium transformation were not affected.

It has been suggested that the Ar_3 temperature of the Nb microalloyed low carbon low alloy steel increased as the amount of dissolved Nb or austenite grain size decreased [10]. On the one hand, the dissolved Nb increases the stability of austenite by decreasing the grain boundary energy as segregating at the austenite grain boundary, and reduces ferrite growth rate due to the solute drag effect as segregating at the austenite/ferrite interphase boundary. On the other hand, Nb precipitates decrease the carbon content in austenite and can act as potential nucleation sites, which promotes ferrite transformation. Furthermore, both the dissolved Nb and Nb precipitates will refine austenite grain size. The decrease of austenite grain size also accelerates ferrite transformation by increasing nucleation rate due to increasing potential nucleation sites. In the present study, at a reheating temperature below 1000 °C, almost all the Nb was precipitated in austenite. At the reheating temperature of 800 °C for annealing or measurement of critical transformation temperatures, the average sizes of austenite grain in the 0.75C-0.04Nb and 0.78C-0.06Nb steels were about half of that in the 0.70C steel. Therefore, the increase of Ar_3 of the Nb microalloyed high carbon steels was mainly attributed to the Nb precipitates and the refinement of austenite grain size. Similar to ferrite transformation, pearlite transformation during continuous cooling in the Nb microalloyed steels would also be promoted at a higher temperature.

4.3. Effects of microalloyed Nb on pearlite spheroidization during continuous cooling

Pearlite spheroidization is thermodynamically driven by the decrease of ferrite/cementite interfacial energy and was considered as a diffusion controlled process [11]. Thus, factors that increase interfacial energy and enhance diffusion will accelerate spheroidization kinetics. The factors included heat treatment temperature, fine pearlite structure, defects in pearlite and the rate controlling element. The spherodization kinetics was controlled by Fe diffusion in ferrite [12] or along ferrite/cementite interface [13]. The microalloyed Nb was largely precipitated and the small amount of dissolved Nb intended to segregate at austenite grain boundary. Therefore, the dissolved Nb hardly influenced the spherodization kinetics. In the present study, pearlite in the 0.75C-0.04Nb and 0.78C-0.06Nb steels began to transform earlier during continuous cooling compared to that in the 0.70C steel, because the Ar_1 temperature in the Nb microalloyed steel was higher. The previously transformed pearlite was firstly spheroidized at a higher temperature. This was the one main reason that spheroidization kinetics became faster after Nb microalloying. The second reason was that the diffusion distance perpendicular to the cementite lamellae was shorter due to smaller interlamellar spacing of pearlite in the 0.75C-0.04Nb and 0.78C-0.06Nb steels. It also increased the driving force of spheroidization by increasing the density of the ferrite/cementite interface. Furthermore, the refinement of pearlite colony size also

reduced the aspect ratio of cementite and the diffusion distance along the cementite lamellae.

Austenite deformation would change the eutectoid point to a higher temperature and higher carbon content by storing deformation energy into austenite [14]. This resulted in increasing spheroidization temperature and a finer pearlite structure. It also transmitted some defects into pearlite to supply rapid diffusion paths. These accounted for the accelerated spheroidization kinetics during on-line spheroidization by hot rolling. In particular, more deformation energy and rapid diffusion paths were stored in the Nb microalloyed steels after hot deformation due to the inhibition effect of Nb on recrystallization. This resulted in the enlarged difference of spherodization among the studied steels after hot deformation. In summary, the acceleration of spherodization kinetics by Nb microalloying during continuous cooling was mainly attributed to the higher transformation temperature, smaller colony size and narrower interlamellar spacing. Hot deformation just above equilibrium eutectoid temperatures accelerated pearlite spheroidization kinetics and gave prominence to the acceleration effect by Nb microalloying.

5. CONCLUSIONS

(1) Compared to the Nb free high carbon steel, Nb microalloyed high carbon steels were refined in the pearlite block, colony and polygonal ferrite grain sizes. Their volume fraction of polygonal ferrite increased, indicating that the carbon content of pearlite exceeded that of pure carbon steels.

(2) The critical temperatures of transformation to ferrite and pearlite during continuous cooling in the Nb microalloyed steels were increased due to the refinement of austenite grain size and the Nb(C,N) precipitates. But the critical temperatures of transformation to austenite during continuous heating were not affected by Nb microalloying.

(3) The degeneracy or partially spherodized area occurred more frequently in the Nb microalloyed steels, mainly attributed to the higher critical transformation temperature and finer pearlite structure with smaller colony size and narrower interlamellar spacing. Hot deformation just above equilibrium eutectoid temperatures accelerated the spheroidization kinetics of pearlite, especially in the niobium microalloyed steels.

ACKNOWLEDGEMENTS

The financial support by the National Basic Research Program of China (973 Program) No. 2010CB630805, the National Natural Science Foundation of China No. 51201036 and CITIC-CBMM R&D project No.2009-292 was gratefully acknowledged.

REFERENCES

1. J. Fu, *Microalloying Tech.* **3-4**, 140 (2009).
2. A. J. DeArdo, *Inter. Mater. Rev.* **48**, 371 (2003).
3. Q. Yong, M. Ma, and B. Wu, *Microalloy Steels-Physical and Mechanical Metallurgy*, pp.1-42, Machinery Industry Press, Beijing (1989).
4. T. Takahashi, M. Nagumo, and Y. Asano, *J. Jpn. Inst. Metals*. **42**, 716 (1978).
5. T. Furuhara, T. Moritani, K. Sakamoto, and T. Maki, *Mater. Sci. For*. **539-543**, 4832 (2007).
6. Z.-D. Li, G. Miyamoto, Z.-G. Yang, and T. Furuhara, *Scr. Mater.* **60**, 485 (2009).
7. E. Cotrina, B. Lopez and J. M. Rodriguez-Ibabe, *Austenite formation and decomposition* (eds. E. B. Damm and M. J. Merwin), pp.213-225, Minerals, Metals & Materials Society, Warrendale (2003).
8. H. I. Aaronson, *Decomposition of Austenite by Diffusional Processes* (eds. V. F. Zackay, and H. I. Aaronson) , pp.387-548, Interscience publishers, New York (1962).
9. N. Ridley, *Metal. Trans. A*. **15A**, 1019 (1984).
10. S. Hong, S. Lim, H. Hong, K. Lee, D. Shin, and K. Lee, *Mater. Sci. Eng. A*. **355**, 241 (2003).
11. G. Krauss, *Steels: Processing, Structure, and Performance*, pp.33-54, Materials Park, Ohio (2005).
12. Y. L. Tian and R. W. Kraft, *Metall. Trans. A*. **15A**, 1359 (1987).
13. O. E. Atasoy and S. Ozbilen, *J. Mater. Sci*. **24**, 281 (1989).
14. Q. Huang, L. Li, W. Yang, and Z. Sun, *Trans. Mater. Heat Treat*. **29**, 45 (2008).